J Solid State Electrochem (2011) 15:2437–2445
DOI 10.1007/s10008-011-1408-6

ORIGINAL PAPER

Pathways of diffusion mixed with subsequent reactions with examples of hydrogen extraction from hydride-forming electrode and oxygen reduction at gas diffusion electrode

Sung-Jai Lee · Su-Il Pyun · Young-Gi Yoon

Received: 19 January 2011 / Revised: 1 March 2011 / Accepted: 3 March 2011 / Published online: 4 May 2011

Abstract This paper covers the role of the rate-determining step (RDS) in anodic hydrogen extraction from hydride-forming electrode. In general, hydrogen extraction from the electrode proceeds through the following steps: (1) hydrogen diffusion within the electrode, (2) hydrogen transfer from absorbed state to adsorbed state, (3) electrochemical oxidation of hydrogen to hydrogen ion involving charge transfer, and (4) hydrogen ion conduction through the electrolyte. In most theoretical and experimental investigations, it has been assumed that the RDS of anodic hydrogen extraction is hydrogen diffusion through the electrode. In real situation, however, the overall rate of hydrogen extraction is simultaneously determined by the rates of two or more reaction steps including hydrogen diffusion. The present work provides the overview of anodic hydrogen extraction in case that diffusion is coupled with interfacial charge transfer, interfacial hydrogen transfer, and hydrogen ion conduction through the electrolyte as well as the purely diffusion-controlled hydrogen extraction. In addition, the mixed controlled diffusion model was also exemplified with oxygen reduction at gas diffusion electrode of fuel cell system.

Keywords Anodic hydrogen extraction · Hydride-forming electrode · Rate-determining step (RDS) · Purely diffusion control · Mixed diffusion control

S.-J. Lee
Fuel Cycle Process Technology Development Division,
Korea Atomic Energy Research Institute,
1045 Daedeok-daero, Yuseong-gu,
Daejeon 305-353, Republic of Korea

S.-I. Pyun (✉)
Department of Materials Science and Engineering,
Korea Advanced Institute of Science and Technology,
291 Daehak-ro, Yuseong-gu,
Daejeon 305-701, Republic of Korea
e-mail: sipyun@kaist.ac.kr

Y.-G. Yoon
Fuel Cell Research Center, Korea Institute of Energy Research,
102 Gajeong-ro, Yuseong-gu,
Daejeon 305-343, Republic of Korea

Introduction

Hydride-forming metals and alloys have been extensively investigated because of their technological applications to electrode materials for rechargeable batteries [1–4]. For several decades, the mechanism of hydrogen insertion into and extraction (desertion) from the hydride-forming electrode has been the main interest to who wants to realize a high-power application. A detailed knowledge of hydrogen insertion and extraction has been acquired by using various electrochemical techniques such as cyclic voltammetry [5, 6], electrochemical impedance spectroscopy [7–11], galvanostatic potential transient technique [12, 13], and potentiostatic current transient (PCT) technique [14–18].

In particular, AC impedance spectroscopy has been widely used to identify the various reaction steps and to determine the rate-determining step (RDS), since it provides an exceptionally powerful tool for separating the dynamics of several electrode processes with different relaxation times [19, 20]. In addition, the PCT technique has proven to be helpful for an understanding of the electrochemical reaction mechanism [4, 21]. The theoretical treatment for the PCT by an analytical calculation allows us to extract quantitative estimates of kinetic parameters for hydrogen extraction.

With few exceptions, most researchers have analyzed their experimental data of current transients for hydrogen extraction

under the assumption of the diffusion-control concept [15–17]. This concept presumes that hydrogen diffusion in the electrode is the RDS of hydrogen extraction. However, various types of abnormalities have frequently appeared in the measured current transients, indicating that a more complicated mechanism may become involved in hydrogen extraction.

The present article discusses the RDS of anodic hydrogen extraction from the hydride-forming electrodes employing both AC impedance spectroscopy and anodic PCT technique. For this purpose, we first derived the theoretical expression for the AC impedance spectra and anodic current transient, then numerically calculated the AC impedance spectra and anodic current for each hydrogen extraction model suggested.

Theoretical analysis of hydrogen extraction under the purely diffusion control

In general, anodic hydrogen extraction from the electrode proceeds through the following steps: (1) hydrogen diffusion within the electrode, (2) hydrogen transfer from absorbed state to adsorbed state, (3) electrochemical oxidation of hydrogen to hydrogen ion involving charge transfer, and (4) hydrogen ion conduction through the electrolyte, which is schematically shown in Fig. 1a.

Under this circumstance, hydrogen extraction can be described by a series of the proton migration resistance R_m, the charge transfer resistance R_{ct}, the hydrogen transfer resistance R_{ht}, and the hydrogen diffusion resistance R_d, which is described in Fig. 1b. Here, a fast reaction step is characterized by a small resistance, while a slow reaction step is represented by a high resistance.

For simplicity, the linear relationship between current I and overpotential η was introduced for each reaction step. When a steady-state condition is attained, the rates of all reaction steps in this series should be the same. Under this condition, η for each reaction step can be written by:

$$\eta_{cm} = I^{st} R_m \tag{1}$$

$$\eta_{ct} = I^{st} R_{ct} \tag{2}$$

$$\eta_{ht} = I^{st} R_{ht} \tag{3}$$

$$\eta_d = I^{st} R_d \tag{4}$$

where I^{st} is the steady-state current.

Summing Eqs. 1–4, one obtains:

$$I^{st} = (\eta_m + \eta_{ct} + \eta_{ht} + \eta_d)/(R_m + R_{ct} + R_{ht} + R_d) \tag{5}$$

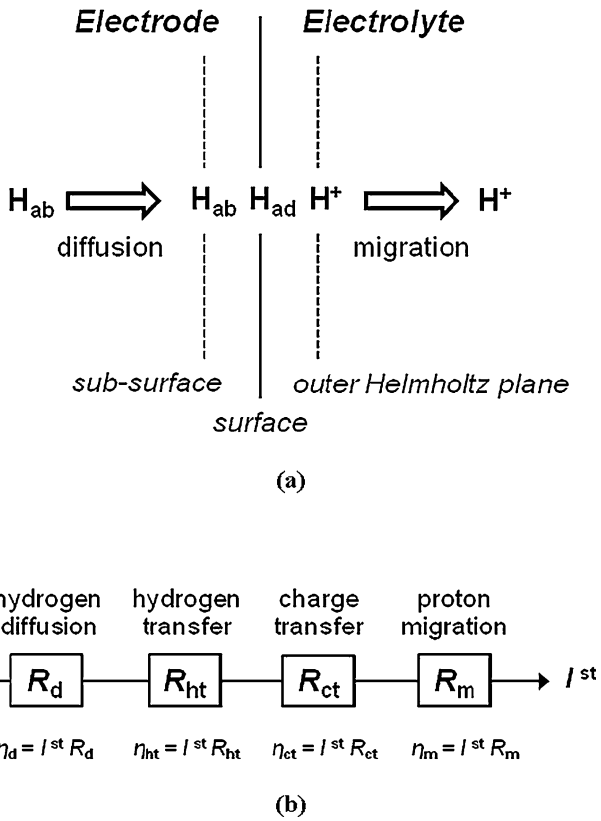

Fig. 1 Schematic diagrams of **a** hydrogen extraction through the hydride-forming electrode and **b** hydrogen extraction from the hydride-forming electrode represented by a series of resistance

Thus, I^{st} is limited by one or more reaction steps with large values of R. Accordingly, the conventional diffusion-controlled hydrogen extraction refers to the condition where R_d exceeds R_m, R_{ct}, and R_{ht} considerably, leading to $\eta_d >> \eta_m$, η_{ct}, and η_{ht}, so that I^{st} is uniquely determined by the resistance of hydrogen diffusion.

To explicitly investigate the role of RDS in hydrogen extraction, the analytical expressions for AC impedance spectra and current transients were determined. Considering the diffusion of the absorbed hydrogen through the membrane under the impermeable boundary condition experimentally accessible, the Faradaic admittance can be derived in the following way. Charge and mass balance give

$$\frac{i_F}{F} = v_1 \qquad \text{(charge balance)} \tag{6}$$

$$\Gamma_{max}\frac{d\theta}{dt} = v_1 - j_{x=0} \qquad \text{(mass balance)} \tag{7}$$

where i_F depicts the Faradaic current, F the Faradaic constant (96,500 C mol^{-1}), v_1 the rate of charge transfer,

Γ_{max} the maximum surface concentration of adsorbed hydrogen, θ the coverage of adsorbed hydrogen, $j_{x=0}$ means the flux of the hydrogen at the surface.

The electrochemical response to sinusoidal oscillation of potential can be expressed in Taylor series expansion. Neglecting the second- and higher-order terms of the series expansion, the sinusoidal response is given by

$$v_1 = v_1^{st} + \left(\frac{\partial v_1}{\partial E}\right)\widetilde{E}\exp(j\omega t) + \left(\frac{\partial v_1}{\partial \theta}\right)\widetilde{\theta}\exp(j\omega t) + \left(\frac{\partial v_1}{\partial c}\right)\widetilde{c}\exp(j\omega t) \tag{8}$$

$$v_2 = v_2^{st} + \left(\frac{\partial v_2}{\partial E}\right)\widetilde{E}\exp(j\omega t) + \left(\frac{\partial v_2}{\partial \theta}\right)\widetilde{\theta}\exp(j\omega t) + \left(\frac{\partial v_2}{\partial c}\right)\widetilde{c}\exp(j\omega t) \tag{9}$$

where v_2 is the rate of hydrogen transfer, v_1^{st} the steady-state rate of charge transfer, v_2^{st} the steady-state rate of hydrogen transfer, E the electrode potential, c the concentration of hydrogen, j the unit of the complex number, i.e., $\sqrt{-1}$, ω the angular frequency, t time, and the superscript ~ means the perturbation due to sinusoidal oscillation.

Considering hydrogen transfer at low hydrogen coverage, the rate of hydrogen transfer is given as

$$v_2 = k_2\theta - k_{-2}c \tag{10}$$

where k_2 is the rate constant of hydrogen transfer from adsorbed state to absorbed state, and k_{-2} is the rate constant of hydrogen transfer from absorbed to adsorbed state.

From the characteristics of Volmer adsorption and Tafel desorption reactions, it is apparent that

$$\left(\frac{\partial v_1}{\partial c}\right) = 0 \tag{11}$$

$$\left(\frac{\partial v_2}{\partial E}\right) = 0 \tag{12}$$

The flux of hydrogen at the surface by sinusoidal oscillation is given by

$$j_{x=0} = \frac{D_H}{L}c^{st} + \sqrt{j\omega D_H}\tanh\left(\sqrt{\frac{j\omega}{D_H}}L\right)\widetilde{c}\exp(j\omega t) \tag{13}$$

where D_H represents the chemical diffusivity of hydrogen, c^{st} the hydrogen concentration in steady-state, and L is the thickness of the electrode.

Substituting Eqs. 8 and 13 into Eqs. 6 and 7 under the reaction constraint given by Eqs. 11 and 12 and equating the time-dependent terms of each other,

$$\frac{\widetilde{i_f}}{F} = \left(\frac{\partial v_1}{\partial E}\right)\widetilde{E} + \left(\frac{\partial v_1}{\partial \theta}\right)\widetilde{\theta} \tag{14}$$

$$j\omega\Gamma_{max}\widetilde{\theta} = \left(\frac{\partial v_1}{\partial E}\right)\widetilde{E} + \left(\frac{\partial v_1}{\partial \theta}\right)\widetilde{\theta} - \sqrt{j\omega D_H} \times \tanh\left(\sqrt{\frac{j\omega}{D_H}}L\right)\widetilde{c} \tag{15}$$

Considering the mass balance between the rate of hydrogen transfer Eqs. 11, 12 and the flux of hydrogen diffusion to the surface Eq. 13, one can obtain

$$\frac{c^{st}}{\theta} = \frac{k_2}{\frac{D_H}{L} + k_{-2}} \qquad \text{at steady} - \text{state} \tag{16}$$

$$\frac{\widetilde{c}}{\widetilde{\theta}} = \frac{\left(\frac{\partial v_2}{\partial \theta}\right)}{-\left(\frac{\partial v_2}{\partial c}\right) + \sqrt{j\omega D_H}\tanh\left(\sqrt{\frac{j\omega}{D_H}}L\right)} \tag{17}$$

Substituting Eq. 17 into Eq. 15, one obtains

$$\frac{\widetilde{\theta}}{\widetilde{E}} = \frac{\left(\frac{\partial v_1}{\partial E}\right)}{j\omega\Gamma_{max} - \left(\frac{\partial v_1}{\partial \theta}\right) + \frac{\left(\frac{\partial v_2}{\partial \theta}\right)}{1 - \frac{\left(\frac{\partial v_2}{\partial c}\right)}{\sqrt{j\omega D_H}\tanh\left(\sqrt{\frac{j\omega}{D_H}}L\right)}}} \tag{18}$$

Substituting $\widetilde{\theta}$ in Eq. 18 into $\widetilde{\theta}$ in Eq. 14, the Faradaic admittance Y_f is determined as

$$Y_f = \frac{\widetilde{i_f}}{\widetilde{E}} = -F\left(\frac{\partial v_1}{\partial E}\right)\left[1 + \frac{\frac{1}{\Gamma_{max}}\left(\frac{\partial v_1}{\partial E}\right)}{j\omega - \frac{1}{\Gamma_{max}}\left(\frac{\partial v_1}{\partial \theta}\right) + \frac{\frac{1}{\Gamma_{max}}\left(\frac{\partial v_2}{\partial \theta}\right)}{1 - \frac{\left(\frac{\partial v_2}{\partial c}\right)}{\sqrt{j\omega D_H}\tanh\left(\sqrt{\frac{j\omega}{D_H}}L\right)}}}\right] \tag{19}$$

One sets

$$R_{ct} = -\frac{1}{F\left(\frac{\partial v_1}{\partial E}\right)}, B = -\left(\frac{\partial v_1}{\partial \Gamma}\right), k_2 = \left(\frac{\partial v_2}{\partial \Gamma}\right), \text{ and } k_{-2} = -\left(\frac{\partial v_2}{\partial c}\right) \tag{20}$$

Equation 14 representing the Faradaic admittance can be converted to impedance equation representing the electrical equivalent circuit,

$$Z_f = \frac{\widetilde{E}}{\widetilde{i}_f} = R_{ct} + \frac{1}{j\omega C_{ht} + \dfrac{1}{R_{ht} + \dfrac{\sigma_W \coth\left(\sqrt{\frac{j\omega}{D_H}}L\right)}{\sqrt{j\omega D_H}}}} \tag{21}$$

where $C_{ht} = -\frac{1}{BR_{ct}}$, $R_{ht} = -\frac{BR_{ct}}{k_2}$, and $\sigma_W = -\frac{k_{-2}}{k_2}BR_{ct}$.

Considering the migration resistance R_m and double layer capacitance C_{dl}, the total impedance Z_{total} is expressed as

$$\begin{aligned} Z_{total} &= R_m + \frac{1}{j\omega C_{dl} + \frac{1}{Z_f}} \\ &= R_m + \frac{1}{j\omega C_{dl} + \dfrac{1}{R_{ct} + \dfrac{1}{j\omega C_{ht} + \dfrac{1}{R_{ht} + \dfrac{\sigma_W \coth\left(\sqrt{\frac{j\omega}{D_H}}L\right)}{\sqrt{j\omega D_H}}}}}} \end{aligned} \tag{22}$$

The equivalent circuit corresponding to Eq. 22 is shown in Fig. 2. Here, it should be noted that the resistances R_m, R_{ht}, R_{ct}, and the Warburg impedance coefficient σ_W are not independent, but closely coupled each other.

A widely held concept in analysis of hydrogen extraction is that hydrogen diffusion in the electrode is the RDS. A more precise description of the diffusion-controlled concept is as follows:

$$Z_{total} = \sigma_W \frac{\coth\left(\sqrt{\frac{j\omega}{D_H}}L\right)}{\sqrt{j\omega D_H}} \tag{23}$$

The Nyquist plot of the AC impedance spectrum calculated from Eq. 23 is shown in Fig. 3a. The impedance spectrum of Fig. 3a consists of a straight line inclined at a constant angle of 45° to the real axis, which represents the Warburg impedance, in the high-frequency range and a capacitive line in the low-frequency range. The Warburg impedance is attributed to the semi-infinite diffusion of hydrogen within the electrode, and the capacitive line is related to the accumulation of hydrogen at the impermeable boundary.

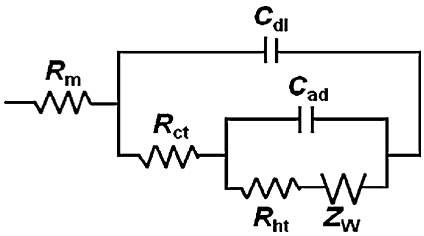

Fig. 2 Equivalent circuit for hydrogen extraction through the hydride-forming electrode

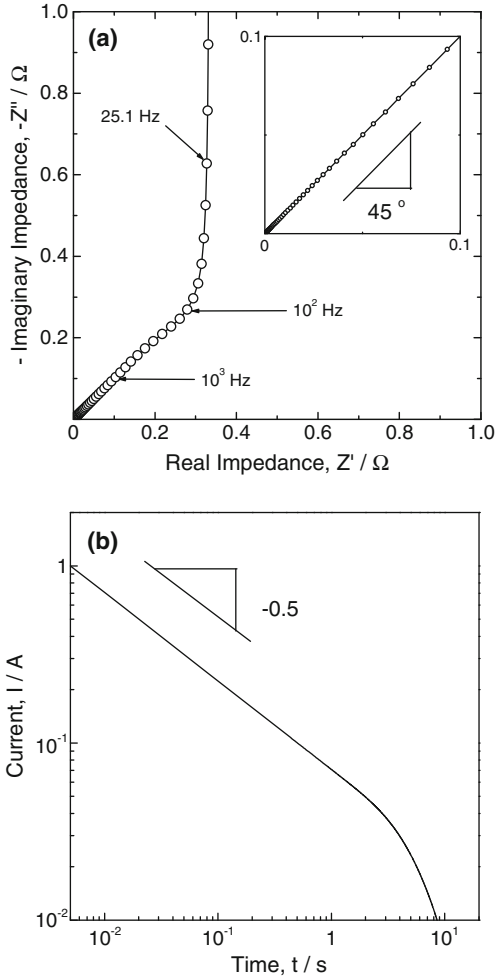

Fig. 3 **a** Nyquist plots of the impedance spectrum and **b** anodic current transient on a logarithmic scale, theoretically determined under the purely diffusion control

In addition, the Laplace transform of the current response $\overline{i(s)}$ to a potential step is related to the impedance by [4, 22]:

$$\overline{i(s)} = \frac{\Delta E}{sZ_{total}(s)} \tag{24}$$

where s represents the Laplace complex variable. The theoretical expression for the PCT can be derived from the inverse Laplace transform of Eq. 24. For the diffusion-controlled hydrogen extraction, the following current–time relation is finally obtained:

$$i = F(c^o - c^s)\left(\frac{D_H}{\pi t}\right)^{1/2} \text{for } i << \frac{L^2}{D_H} \tag{25}$$

$$i = \frac{2F(c^o - c^s)D_H}{L}\exp\left(-\frac{\pi^2 D_H}{4L^2}t\right) \text{for } i >> \frac{L^2}{D_H} \tag{26}$$

where c^o and c^s denote the initial equilibrium concentration and the surface concentration of hydrogen, respectively.

Figure 3b illustrates the anodic current transient on a logarithmic scale numerically calculated from Eqs. 25 and 26 under the pure diffusion control. The simulated current transient clearly exhibits a linear relationship between the logarithm of current and the logarithm of time with an absolute slope of 0.5, which represents the Cottrell behavior, followed by an exponential decay of current with time, as predicted from Eqs. 25 and 26.

Hydrogen extraction under the mixed control

Most of the electrochemical experiments from hydride-forming electrodes have been analyzed by employing the diffusion-controlled concept described in the previous section. However, anomalous behaviors of several types showing a strong deviation from the diffusion-control model have frequently been observed.

The abnormality in the current transients commonly observed is that the slope of the logarithmic current transient is lower in absolute value than 0.5 in the early stage. The anomalous behaviors in hydrogen extraction from various hydride-forming electrodes have been independently explored by several research groups [23–26].

Especially, Pyun and coworkers have made an exhaustive study into anomalous hydrogen extraction in hydride-forming electrodes [21, 27–31]. From the analyses of the experimental and theoretical current transients, it is suggested that the diffusion-controlled constraint is scarcely satisfied at the electrode surface, when hydrogen diffusion proceeds under the dominant influences of the proton migration, charge transfer, or hydrogen transfer reactions.

Diffusion coupled with charge transfer

One of the basic premises of the diffusion-control model is that the charge transfer reaction on the electrode surface is too facile to affect hydrogen extraction. However, there is much experimental evidence indicating that the charge transfer rate is not sufficiently fast to maintain the validity of such assumption. As a matter of fact, many of the AC impedance results from hydride-forming electrodes suggested the presence of a large interfacial charge transfer resistance, which implies slow charge transfer kinetics [8, 9].

In those cases, it is plausible that both hydrogen diffusion and interfacial charge transfer are markedly disturbed from the equilibria, thereby hydrogen diffusion and interfacial charge transfer become simultaneously involved in the RDSs of hydrogen extraction. This means that hydrogen extraction proceeds under the constraint of hydrogen diffusion mixed with interfacial charge transfer.

In the case of hydrogen extraction under the mixed control of hydrogen diffusion and charge transfer, the analytical expression for impedance spectra were derived by assuming that both hydrogen diffusion and charge transfer control the rate of the overall reaction. A more precise description of this concept is as follows:

$$Z_{\text{total}} = \frac{1}{j\omega C_{\text{dl}} + \dfrac{\sqrt{j\omega D_{\text{H}}}}{R_{\text{ct}}\sqrt{j\omega D_{\text{H}}} + \sigma_{\text{W}} \coth\left(\sqrt{\frac{j\omega}{D_{\text{H}}}} L\right)}} \tag{27}$$

The Nyquist plot of the AC impedance spectra calculated from Eq. 27 is shown in Fig. 4a. It is found in Fig. 4a that all the calculated impedance spectra is composed of an arc in the high-frequency range, a straight line inclined at a constant angle of 45° to the real axis in the intermediate frequency range, and a capacitive line in the low-frequency range. From the fact that the size of the high-frequency arc increased with increasing charge transfer resistance, it is

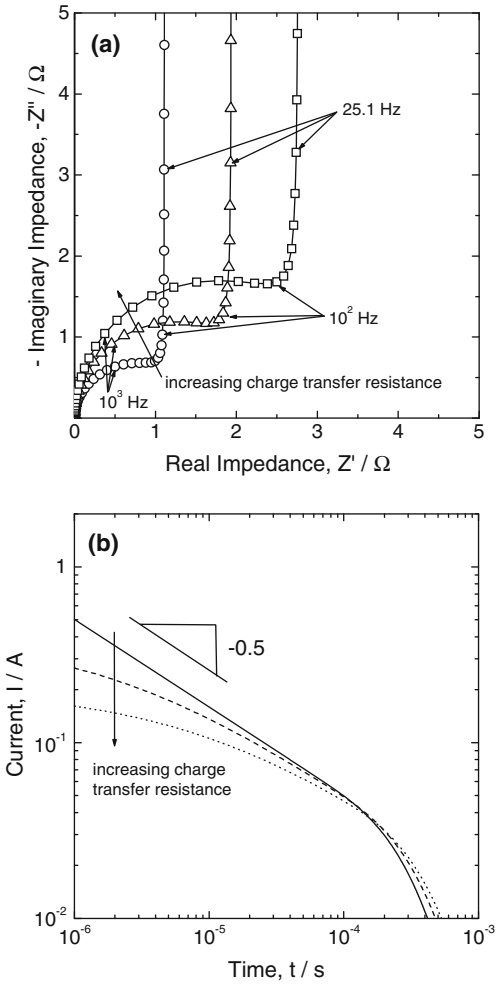

Fig. 4 **a** Nyquist plots of the impedance spectra and **b** anodic current transients on a logarithmic scale, theoretically determined as a function of the charge transfer resistance under the mixed control of hydrogen diffusion and charge transfer

confirmed that the high-frequency arc is closely related to charge transfer.

The theoretical expression for the PCT can be derived from the inverse Laplace transform of Eq. 27. For the mixed control of hydrogen diffusion and charge transfer, the following current–time relation is obtained:

$$i = \frac{2F(c^{o} - c^{s})D_{H}}{L} \times \sum_{n=1}^{\infty} \frac{\Lambda^2}{\Lambda^2 + \Lambda + b_n^2} \exp\left(-\frac{b_n^2 D_H}{L^2} t\right) \quad (28)$$

where Λ is the dimensionless parameter denoting the ratio of the diffusion resistance R_d to the charge transfer resistance R_{ct} ($\Lambda = R_d/R_{ct}$) and b_n is the nth positive root of ($b \tan b - \Lambda = 0$).

Figure 4b gives on a logarithmic scale the anodic current transient numerically determined from Eq. 28 as a function of the charge transfer resistance. The simulated current transients deviated from the Cottrell behavior in the case of a large charge transfer resistance, and the deviation from the Cottrell behavior grew up with rising charge transfer resistance.

Here, it should be stressed that the shape and value of the current transient are highly dependent on the potential step. The initial current at $t=0$ rises exponentially with increasing potential step, represented by the Butler–Volmer equation. Hence, the linear relationship between the logarithmic initial current and the potential step is one of the decisive experimental evidences.

Diffusion coupled with hydrogen transfer

Investigations of some metal hydrides such as Pt, Pd, and Ni single crystal surfaces [32, 33] have indicated the existence of absorbed state for hydrogen at the electrode subsurface which represents hydrogen atom residing just beneath the surface layer of the metal. In the case of hydride-forming metals which are capable of absorbing hydrogen, therefore, hydrogen transfer between H_{ad} on the electrode surface and H_{ab} at the electrode subsurface has been considered to be one of the essential steps for hydrogen extraction. Actually, its role in hydrogen extraction has been discussed in several theoretical models and evidenced experimentally [34].

To the best of our knowledge, Yang et al. [35, 36] first carried out the systematic studies on hydrogen extraction under the influence of the hydrogen transfer reaction by using galvanostatic potential transient method. In their works, the theoretical formulations were made for the galvanostatic discharge process including hydrogen diffusion followed by the hydrogen transfer reaction, and the experimental data obtained from the Zr-based amorphous alloys were found to be successfully explained by the theoretical model derived.

In the study of hydrogen extraction under the mixed control of hydrogen diffusion and hydrogen transfer, the impedance spectra were analyzed by assuming that hydrogen diffusion and hydrogen transfer control the rate of the overall reaction. A more precise description of this concept is as follows:

$$Z_{total} = \frac{1}{j\omega C_{ht} + \frac{\sqrt{j\omega D_H}}{R_{ht}\sqrt{j\omega D_H} + \sigma_W \coth\left(\sqrt{\frac{j\omega}{D_H}} L\right)}} \quad (29)$$

The Nyquist plot of the AC impedance spectra calculated from Eq. 29 is shown in Fig. 5a. Similar to Fig. 4a, all the calculated impedance spectra is composed of an arc in the high-frequency range, a straight line inclined at a

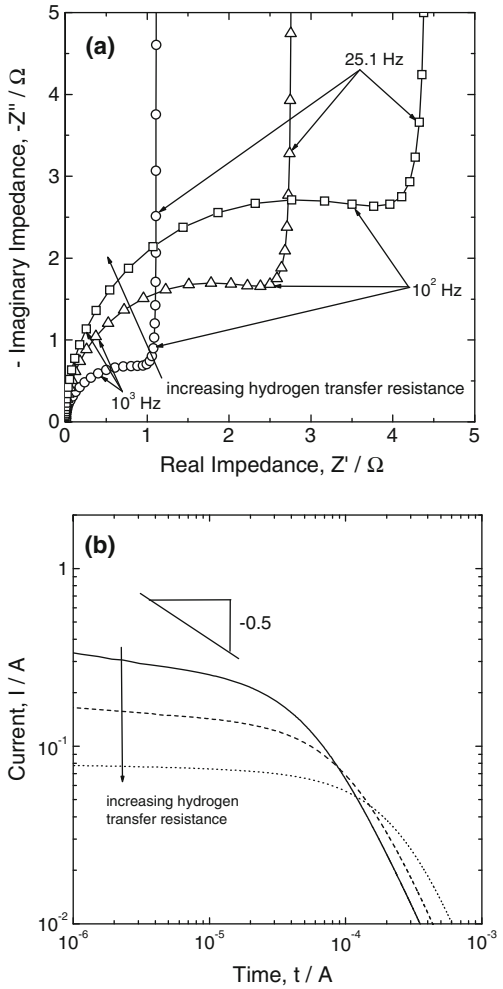

Fig. 5 **a** Nyquist plots of the impedance spectra and **b** anodic current transients on a logarithmic scale, theoretically determined as a function of the hydrogen transfer resistance under the mixed control of hydrogen diffusion and hydrogen transfer

constant angle of 45° to the real axis in the intermediate frequency range, and a capacitive line in the low-frequency range in the same manner as the mixed control of hydrogen diffusion and charge transfer. However, the high-frequency arc is attributed to hydrogen transfer rather than charge transfer; hence, as the hydrogen transfer resistance increased, the size of the high-frequency arc also increased.

The theoretical expression for the PCT can be also derived from the inverse Laplace transform of Eq. 29. For the mixed control of hydrogen diffusion and hydrogen transfer, the following current–time relation is obtained by assuming that charge transfer is so facile that the adsorbed hydrogen on the electrode surface is immediately oxidized; hence, the value of θ approaches zero:

$$i=F\left(\frac{k_2}{\Gamma_{\max}}\right)c^o \exp\left[\left(\frac{k_2}{\Gamma_{\max}}\right)^2 \frac{t}{D_H}\right]\mathrm{erfc}\left[\frac{k_2}{\Gamma_{\max}}\left(\frac{t}{D_H}\right)^{1/2}\right] \quad (30)$$

Figure 5b gives on a logarithmic scale the anodic current transient numerically determined from Eq. 30 with respect to the hydrogen transfer resistance. All of the simulated current transients hardly follow the Cottrell behavior, i.e., the logarithmic current transient runs with an absolute slope flatter than 0.5. In addition, the absolute slope of current transient decreased with increasing hydrogen transfer resistance.

However, the logarithm of the initial current at $t=0$ shares the almost constant value irrespective of the potential step. From the fact that the anodic current transient shows non-Cottrell behavior, but the initial current remains nearly constant regardless of the potential step, it is conceivable that hydrogen extraction from the hydride-forming electrode proceeds under the mixed control of hydrogen diffusion and hydrogen transfer.

Diffusion coupled with hydrogen ion conduction

In literature [29], the anodic current transients measured in the electrochemical cells with various distances d between the working and reference electrodes. As the value of d decreased, the absolute slope of the logarithmic current transient increased from 0 to 0.5. It is generally known that the proton migration resistance R_m is linearly proportional to the value of d in a planar configuration of the electrochemical cell.

Bearing in mind that the logarithmic current transient exhibits an absolute slope being close to zero for a large value of R_m, it is reasonable that the current plateau is attributed to simultaneously effects of hydrogen diffusion and proton migration on hydrogen extraction.

The impedance spectra of hydrogen extraction under the mixed control of hydrogen diffusion and proton migration were analyzed by assuming that hydrogen extraction proceeds under the condition where hydrogen diffusion is mixed with proton migration. A more precise description of this concept is as follows:

$$Z_{\text{total}} = R_m + \sigma_W \frac{\coth\left(\sqrt{\frac{j\omega}{D_H}}L\right)}{\sqrt{j\omega D_H}} \quad (31)$$

The Nyquist plot of the AC impedance spectra calculated from Eq. 31 is shown in Fig. 6a. It is found in Fig. 6a that all the calculated impedance spectra is composed of a straight line inclined at a constant angle of 45° to the real axis in the high-frequency range and a capacitive line in the low-frequency range in the same manner of the purely diffusion control. However, the intersection of the straight line with the real axis moved away from the origin as the migration resistance increased.

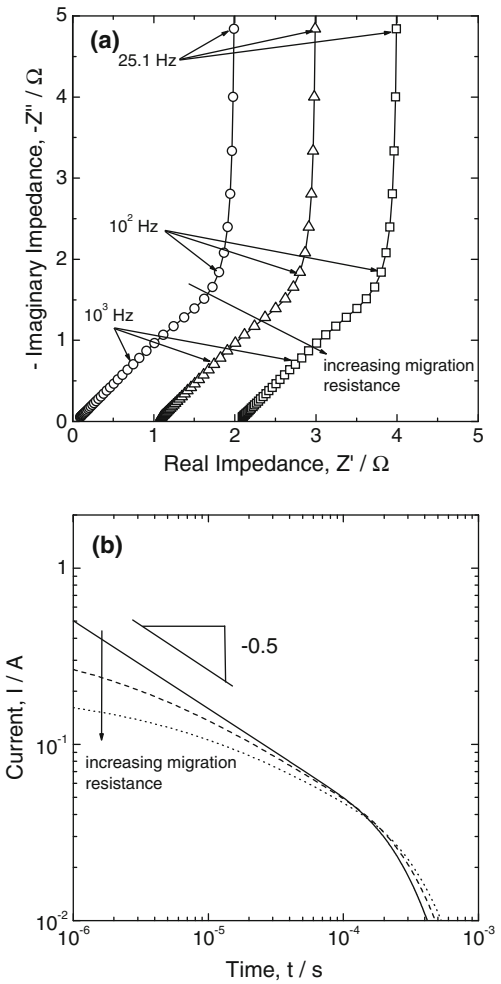

Fig. 6 **a** Nyquist plots of the impedance spectra and **b** anodic current transients on a logarithmic scale, theoretically determined as a function of the migration resistance under the mixed control of hydrogen diffusion and proton migration

The theoretical expression for the PCT can be also derived from the inverse Laplace transform of Eq. 31. For the mixed control of hydrogen diffusion and hydrogen transfer, the following current–time relation is obtained:

$$i = \frac{2F(c^{o} - c^{s})D_{H}}{L} \times \sum_{n=1}^{\infty} \frac{\Lambda^2}{\Lambda^2 + \Lambda + b_n^2} \exp\left(-\frac{b_n^2 D_H}{L^2} t\right) \quad (32)$$

Here, it should be noted that Λ is defined as the ratio of the diffusion resistance R_d to the proton resistance R_m ($\Lambda = R_d/R_m$) rather than the charge transfer resistance R_{ct} in Eq. 28.

Figure 6b gives on a logarithmic scale the anodic current transient numerically determined from Eq. 32 as a function of the migration resistance. Similar to the mixed hydrogen diffusion and charge transfer, the larger the proton migration resistance, the more the deviation from the Cottrell behavior. Furthermore, the relationship between the logarithm of the initial current at $t=0$ and the potential step shows the same tendency as the mixed control of hydrogen diffusion and charge transfer.

Application of mixed diffusion control theory to analysis of overall oxygen reduction in fuel cell system

The mixed diffusion control theory can be extended to the electrochemical reaction in fuel cell which occurs under the constraint of the mixed control of proton migration and charge transfer. Many researchers have reported that the overall oxygen reduction reaction in the gas diffusion electrode proceeds under the condition where proton transport through the Nafion electrolyte is kinetically mixed with the charge transfer reaction at the three-phase boundary [37, 38].

The systematic studies on oxygen reduction under the mixed diffusion control have been carried out by Pyun and coworkers employing potentiostatic current transient technique and AC impedance spectroscopy [39–44]. In their works, the analytical expressions of the current transient and impedance spectrum were derived under the mixed control, and the experimental evidences were found to be successfully explained by the theoretical model derived.

In the study of oxygen reduction in fuel cell condition under the mixed control of proton migration and charge transfer, the impedance spectra were analyzed as follows:

$$Z_{total} = \left(\frac{R_m R_{ct}}{1 + j\omega R_{ct} C_{dl}}\right)^{1/2} \coth\left[L\left(\frac{R_m}{R_{ct}}\right)^{1/2} (1 + j\omega R_{ct} C_{dl})^{1/2}\right] \quad (33)$$

The Nyquist plot of the AC impedance spectrum calculated from Eq. 33 is shown in Fig. 7a. The measured impedance spectrum consists of a straight line inclined at a constant angle of 45° to the real axis in the high-frequency range and a depressed arc in the low-frequency range. Here, the straight line in the high-frequency range is attributable to proton transport through the Nafion electrolyte and the low-frequency arc is due to the charge transfer reaction at the three-phase boundary.

The theoretical expression for the PCT can be derived from the inverse Laplace transform of Eq. 33 as follows:

$$I(t) = \frac{2\Delta E}{R_m} \sum_{n=1}^{\infty} \frac{\Lambda}{\Lambda^2 + \Lambda + b_n^2} \exp\left(\frac{b_n^2}{R_{ct} C_{dl} L^2} t\right) \quad (34)$$

Figure 7b gives on a logarithmic scale the anodic current transient numerically determined from Eq. 34. The logarithmic current transient runs with an absolute slope flatter than 0.5.

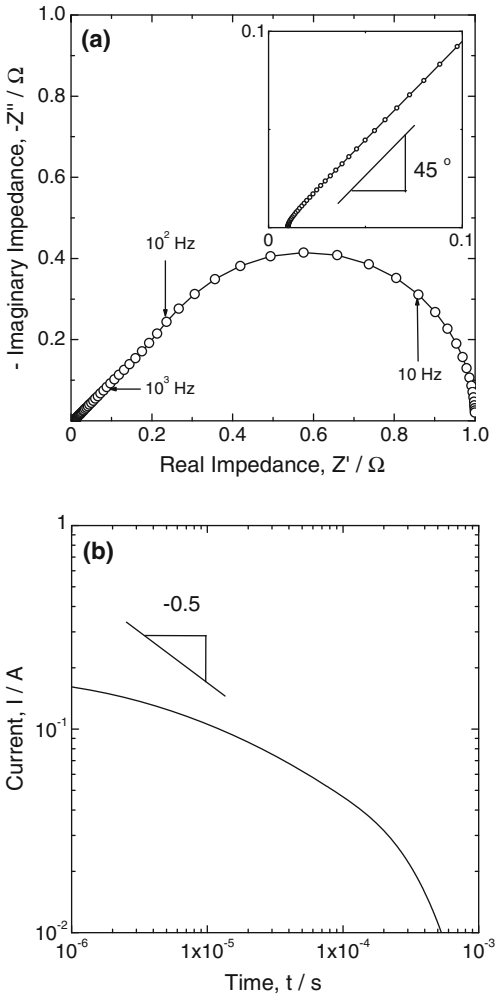

Fig. 7 **a** Nyquist plots of the impedance spectrum and **b** anodic current transient on a logarithmic scale, theoretically determined under the mixed control of proton migration and interfacial charge transfer at the three-phase boundary of fuel cell

Concluding remarks

The present work provides the overview of anodic hydrogen extraction from the hydride-forming electrode in case that diffusion is coupled with interfacial charge transfer, interfacial hydrogen transfer, and hydrogen ion conduction through the electrolyte as well as the purely diffusion-controlled hydrogen extraction. The theoretical expressions of the AC impedance spectra and anodic current transient were first derived for each hydrogen extraction model suggested. Then, the AC impedance spectra and anodic current transient were analyzed as a function of each resistance. Furthermore, the given model was readily applied further to oxygen reduction at the gas diffusion electrode.

In this study, only four kinds of RDSs, i.e., purely diffusion control and three mixed diffusion controls, are considered. However, hydrogen extraction and oxygen reduction proceed in the presence of structural defects in real multiphase system in complex ways as well; hence, it is conceivably expected that three or more reaction steps simultaneously determine the overall hydrogen extraction and oxygen reduction. These problems are still open to solve.

Acknowledgements One of the authors (S-JL) greatly appreciates the support of the Ministry of Education, Science, and Technology. This research is implemented as part of the National Mid- and Long-term Atomic Energy R&D Program, which is supported by the Ministry of Education, Science and Technology. This paper is dedicated to Professor George Inzelt, who pioneered advances in electrochemistry, on the occasion of the 65th anniversary of his birth.

References

1. Fuller TF, Newman J (1995) Metal hydride electrodes. In: White RE, Bockris JO'M, Conway BE (eds) Modern aspects of electrochemistry, vol 27. Plenum, New York, pp 359–382
2. Feng F, Geng M, Northwood DO (2001) Int J Hydrogen Energy 26:725–734
3. Wronski ZS (2001) Int Mater Rev 46:1–49
4. Lee JW, Pyun SI (2005) Electrochim Acta 50:1777–1805
5. Han JN, Lee JW, Seo M, Pyun SI (2001) J Electroanal Chem 506:1–10
6. Gamboa SA, Sebastian PJ, Feng F, Geng M, Northwood DO (2002) J Electrochem Soc 149:A137–A139
7. Lim C, Pyun SI, Ju JB (1991) J Alloy Comp 176:97–103
8. Yoon YG, Pyun SI (1995) Electrochim Acta 40:999–1004
9. Yang TH, Pyun SI (1996) Electrochim Acta 41:843–848
10. Montella C (1999) J Electroanal Chem 462:73–87
11. Georen P, Hjelm AK, Lindbergh G, Lundqvist A (2003) J Electrochem Soc 150:A234–A241
12. Haran BS, Popov BN, White RE (1998) J Electrochem Soc 145:4082–4090
13. Feng F, Ping X, Zhou Z, Geng M, Han J, Northwood DO (1998) Int J Hydrogen Energy 23:599–602
14. Conway BE, Wojtowicz J (1992) J Electroanal Chem 326:277–297
15. Ura H, Nishina T, Uchida I (1995) J Electroanal Chem 396:169–173
16. Kim HS, Nishizawa M, Uchida I (1999) Electrochim Acta 45:483–488
17. Yuan X, Xu N (2001) J Appl Electrochem 31:1033–1039
18. Kim HS, Itoh T, Nishizawa M, Mohamedi M, Umeda M, Uchida I (2002) Int J Hydrogen Energy 27:295–300
19. Lim C, Pyun SI (1993) Electrochim Acta 38:2645–2652
20. Barsoukov E, Macdonald JR (eds) (2005) Impedance spectroscopy: theory, experiment, and applicatons. Wiley, Hoboken, New Jersey, pp 15–54
21. Lee SJ, Pyun SI, Lee JW (2005) Electrochim Acta 50:1121–1130
22. Montella C, Michel R, Diard JP (2007) J Electroanal Chem 608:37–46
23. Iino M (1982) Acta Matall 30:367–375
24. Chen JS, Diard JP, Durand R, Montella C (1996) J Electroanal Chem 406:1–13
25. Lundqvist A, Lindbergh G (1998) J Electrochem Soc 145:3740–3746
26. Millet P, Srour M, Faure R, Durand R (2001) Electrochem Commun 3:478–482
27. Yang TH, Pyun SI, Yoon YG (1997) Electrochim Acta 42:1701–1708
28. Yoon YG, Pyun SI (1997) Electrochim Acta 42:2465–2474
29. Han JN, Seo M, Pyun SI (2001) J Electroanal Chem 499:152–160
30. Pyun SI, Lee JW, Han JN (2002) J New Mater Electrochem Syst 5:243–249
31. Lee JW, Pyun SI, Filipek S (2003) Electrochim Acta 48:1603–1611
32. Eberhardt W, Greuter F, Plummer EW (1981) Phys Rev Lett 46:1085–1088
33. Felter TE, Foiles SM, Daw MS, Stulen RH (1986) Surf Sci 171: L379–L386
34. Lasia A, Gregoire D (1995) J Electrochem Soc 142:3393–3399
35. Yang QM, Ciureanu M, Ryan DH, Strom-Olsen JO (1994) J Electrochem Soc 141:2108–2112
36. Yang QM, Ciureanu M, Ryan DH, Strom-Olsen JO (1994) J Electrochem Soc 141:2113–2117
37. Eikerling M, Kornyshev AA (1999) J Electroanal Chem 475:107–123
38. Makharia R, Mathias MF, Baker DR (2005) J Electrochem Soc 152:A970–A977
39. Kim YM, Pyun SI, Kim JS, Lee GJ (2007) J Electrochem Soc 154:B802–B809
40. Lee SJ, Pyun SI (2007) Electrochim Acta 52:6525–6533
41. Lee SK, Pyun SI, Lee SJ, Jung KN (2007) Electrochim Acta 53:740–751
42. Kim JS, Pyun SI, Shin HC, Kang SJL (2008) J Electrochem Soc 155:B762–B769
43. Kim JS, Pyun SI (2009) Electrochim Acta 54:952–960
44. Lee SJ, Pyun SI (2010) J Solid State Electrochem 14:775–786